

Small Diameter Tubular Structure Design Using Solvent-Free Textile Techniques

Olga Chrzanowska, Marcin Henryk Struszczyk, Izabella Krucinska

Centre of Advanced Technologies of Human-Friendly Textiles "Pro Humano Tex," Department of Material and Commodity Sciences and Textile Metrology, Faculty of Material Technologies and Textile Design, Lodz University of Technology, 90-924 Lodz, Poland
Correspondence to: O. Chrzanowska (E-mail: olga.mazalewska@p.lodz.pl)

ABSTRACT: The aim of research was to elaborate the non-biodegradable (made of polypropylene (PP)) and resorbable (made of polylactide (PLA)) tubular fibrous structures for the reconstruction of the vascular vessels. For the mentioned structures design, nonconventional manufacturing techniques such as melt blown, melt electrospinning, and melt electroblowing were used. Three techniques were chosen as methods allowing on the fibrous structures manufacture containing fibers in nano- or submicro-size diameter. Other advantages of free-solvent technique use is the reduction in the clinical adverse events associated with solvent resided in the fibrous structure during the fabrication. The tubular fibrous structures of PP and PLA using above-mentioned techniques were designed. In first stage, the analysis of the processing parameters influence on the nonbiodegradable and biodegradable tubular structures fiber diameter was performed. Subsequently, the validation step was the analysis of the influence of processing parameters on PP and PLA structural properties for each manufacturing techniques was investigated. The research results confirmed the ability of the tubular structures manufacture with various fiber diameter depending on the applied technique and processing parameters. © 2013 Wiley Periodicals, Inc. *J. Appl. Polym. Sci.* **2014**, *131*, 40147.

KEYWORDS: biomedical applications; biomaterials; differential scanning calorimetry (DSC); spectroscopy

Received 17 May 2013; accepted 30 October 2013

DOI: 10.1002/app.40147

INTRODUCTION

The cardiovascular therapies used to treat occluded vessels are supported by invasive procedures such as surgical bypass and autologous grafting or minimally invasive surgery using endoprosthesis techniques such as intravascular stents. Bypass surgery is the most common surgical intervention for coronary and peripheral atherosclerotic disease, with at least 500,000 bypasses performed annually.¹

Vascular prostheses made of porous fabrics such as expanded polytetrafluoroethylene (Teflon[®]) and woven or knitted polyethylene terephthalate (Dacron[®]) are clinically available for reconstructions of high diameter arteries (within an internal diameter of more than 10 mm).² In addition, it has been demonstrated that small diameter grafts of Dacron[®] failed rapidly because of a high occlusion rate, making only large diameter grafts suitable for use. Expandable Teflon[®] (ePTFE) grafts are more suitable for reconstructions of small diameter blood vessels; however, their structure does not promote tissue in-growth and integration with the host tissue.²⁻⁴

Therefore, new approaches for the manufacture of small diameter vascular prostheses are still warranted. There is an active

challenge for the design of a tubular structure with an inertial diameter less than 6 mm and clinical success in terms of low blood flow rate configurations, reducing anastomotic hyperplasia and promoting a thin, stable, mature neointima formation onto the luminal surface of artificial grafts.⁵

Gulbins et al. and Moreno et al. examined the application of melt blowing techniques for the design of vascular prostheses.⁶⁻⁸ Gulbins manufactured the vascular grafts by blowing melted polyurethane.⁷ The study yielded elaborate structures consisting of 10 to 50 μm thick polymer fibers that were suitable for cell attachment, especially for fibroblasts and smooth muscle cells. However, Moreno et al.⁸ investigated nonwoven fibrous scaffolds originated from melt-blown polyethylene terephthalate fibers, with the diameter of the smallest fiber ranging from 1 to 5 μm , and the pore size distributed from 1 to 20 μm . The biomechanical and biocompatible properties of the scaffolds were analyzed. Above-mentioned research presents the preliminary potentiality of melt blown tubular structures with micro fiber diameter design for the application as the vascular scaffolds.

Widely investigated techniques for the biomaterials fabrication are solution or melt electrospinning.⁹⁻¹¹ The increasing interest

of solvent-free electrospinning application for the production of biomimetic structures for possible medical applications, i.e., tissue engineering is noticeable. Several researchers have used a combination of the solution electrospinning with melt electrospinning or melt spinning/electrospinning with a direct writing mode to produce biomedical devices.^{11–14}

The applied hybrid electrospinning process for the nano-/micro-fibrous 3-D scaffolds design of poly(D,L-lactide-co-glycolide) – (PLGA) were presented by Kim et al.¹² The hybrid electrospinning process was developed by combining melt electrospinning with solution electrospinning. The designed structures have been used as a potential material for skin regeneration.

Chung et al.¹¹ made porous and biodegradable multilayered tubular structures using the elastomeric poly-(L-lactide-co-caprolactone) with the combination of melt spinning and solution electrospinning to form the separate scaffold layers.

The other method of tubular structures manufacturing was presented by Brown et al.¹³ They developed a polycaprolactone melt electrospinning involving a direct writing mode.¹³ The resulting tubes were designed using 20 μm diameter fibers with controllable micro-patterns and mechanical properties.

The aim of the research is construction of multilayered vascular prostheses consisting in the inert and external layer being made of resorbable polymer - polylactide (PLA) and middle layer of nonbiodegradable polymer - polypropylene (PP). The concept of multilayered vascular prostheses design has been presented in previous publication.¹⁵

The current stage of research is to develop the small diameter tubular fibrous structures using melt blowing and melt electrospinning and using a combination of both techniques. The non-solvent techniques use is advantageous for the vascular prosthesis formation due to reduction of solvent residue induced toxicity negatively influencing tissue in-growth. Each of the techniques was based on the melting and feeding of a thermoplastic polymer through a spinning extruder head. The melt blowing process enables the production of nonwovens directly from thermoplastic polymers using compressed air. In the melt blowing process, compressed, hot air blows a molten resin from the extruder die tip onto a collector mandrel to form thin fibers.¹⁶ However, electrostatic forces affect the molten polymer in the melt electrospinning process as the spinning extruder head forms a cone shaped polymer from which small polymer jets eject.¹⁷ The third method, melt electroblowing, is a melt electrospinning process assisted with blowing air. In this process, two applied forces connected with an electrical input and blowing air interact through shear forces to fabricate thin fibers from the polymeric fluid.¹⁷

The influence of processing parameters for each melt technique on the resulting fiber diameter and physicochemical parameters of the tubular fibrous structures was analyzed. The obtained results will provide a basis for analyzing the mechanical and physical properties of melt blown, melt electrospun, or melt electroblown originated tubular structures. In addition, the investigation allow for the selection of the most appropriate technology and processing parameters for multilayered tubular structure design. Moreover, this study is beneficial for the potential appli-

cation in the cardiovascular implants area, including small diameter (less than 6 mm) blood vessel replacements.

Polymers for the resorbable and nonbiodegradable tubular structure design were selected based on preliminary research on flat structures. The selection of suitable polymers were based on analysis of the effect of the rheological parameters and the processing parameters of melt electrospinning on the fiber diameter, and on the physical and structural properties of resulting flat structures. The conduct of this stage of the research was presented at previous publications.^{15,18–21} Polymers used for the fabrication of the nonbiodegradable and biodegradable tubular structures were chosen based on:

- biocompatibility and biodegradation aspects (clinical compliance aspect)
- appropriate properties for the melt technique (technological aspect)
- thin fiber formation with high repeatability (quality and quantity aspect)

Three PP granulates of different melt flow rates (3.4 g/10 min, 25 g/10 min, or 450 g/10 min) were selected for the study of flat non-biodegradable fibrous structures.²² Amorphous and semicrystalline PLAs were also selected for the biodegradable flat structure design. Moreover, the melt electrospinning of the flat fibrous structures was performed for each polymer – PP and PLA.

The flat fibrous structures originated from PP granulate (MFR of 25 g/10 min), and flat structures of amorphous PLA were characterized by the lowest fiber diameter and with the highest repeatability of all studied polymers. These two polymers were selected for tubular structures manufacturing.

The preliminary stage of the research based on flat structures fabrication from three types of PP or two types of PLA granulates allowed screening the most optimal polymer for the elaboration of biodegradable or nondegradable structure and performing the preliminary optimization of melt electrospinning process. The results of the screening and optimization process were presented in the previous publications.^{15,20,21}

The optimum structure will enable cells to proliferate and will also facilitate the delivery of oxygen and nutrient diffusion.²³

A key design consideration of artificial prostheses is the integration of interconnected pores that generate high porosity to promote cell–cell and cell–matrix communication and simultaneously possess sufficient mechanical properties to counteract blood pressure effects.²⁴

MATERIALS AND METHODS

Materials

Materials Used for Designing the Nonbiodegradable Fibrous Structures. Moplen HP 462R PP was obtained from Basell Orlen Polyolefins, Poland.

The polymer manufacturer provides MFR values of Moplen HP 462R PP (25 g/10 min) determined according to the ISO 1133:2011 Standard. The melt temperature was 162°C (determined by DSC according to the PN-EN ISO 1135: 2009 Standard).

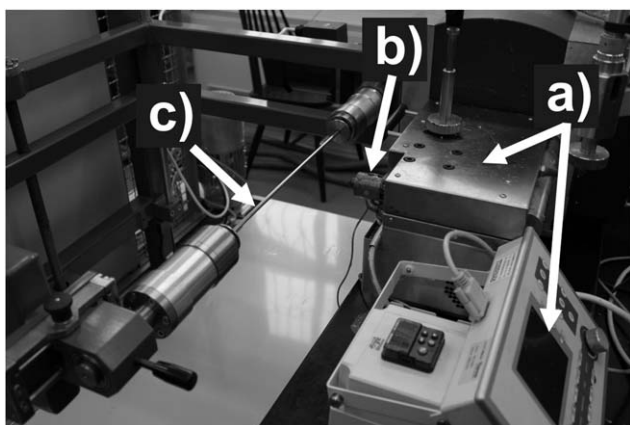


Figure 1. The tubular structure processing system: (a) MiniLab, (b) spinning head, (c) collector mandrel.

Materials Used for Fabricating Biodegradable Fibrous Structures. PLA (PLA 4060D) was purchased from Nature Works LLC, USA. The number average molecular weight for PLA 4060D was 87 kDa.²⁵ According to the specification sheet provided by the polymer manufacturer, the amorphous PLA

contains 88.0% L-lactide and 12.0% D-lactide.²⁶ The seal initial temperature was 80°C (determined by Vicat method according to the PN – EN ISO 306: 2006 Standard).

Methods

The melt blowing, melt electrospinning, and melt electroblowing of the tubular structures were performed using an EX-16H (Zamak/Poland) and MiniLab (Haake/Germany) twin-screw extruder and a rotating collector with a mandrel measuring 5 mm in diameter.

A spinning extruder head with a compressed air adapter, which allows the manufacture of melt blown and melt electrospinning nonwovens, was specially designed for and used on the MiniLab extruder.

The heating zone of the MiniLab extruder reduced the time the polymer had to reside in the extruder working space and permitted the processing of polymers with higher melting temperatures (PLA 4060D). Figure 1 shows the processing system used for the tubular structure fabrication.

The processing parameters of each technique used for both polymers, PP or PLA, are shown in Table I.

Table I. Processing Parameters of Each Used Technique for PLA or PP

Melt blown						
Type of polymer	Extruder processing parameters				Collector processing parameters	
	Head temperature (°C)	Twist of screws (rpm)	Distance between collector and spinneret (cm)	Air flow rate (Nm ³ /h)	Speed of spindle (rpm)	Speed of oscillation (mm/s)
Moplen HP 462R PP	290	0.1 or 0.5	15	5, 10, 20, 30, or 40	11	30 or 15
PLA 4060D	190, 210 or 220	1.0	15	20, 30, or 40	11 or 6	30

Melt electrospinning						
Type of polymer	Extruder processing parameters				Collector processing parameters	
	Head temperature (°C)	Twist of screws (rpm)	Distance between collector and spinneret (cm)	Spinning voltage (kV)	Speed of spindle (rpm)	Speed of oscillation (mm/s)
Moplen HP 462R PP	270, 290, or 300	0.1, 0.5, or 1	4 or 15	35–40	11	30
PLA 4060D	170, 180, 190, 200, or 220	0.1	6 or 10	30–37	11	30

Melt electroblowing							
Type of polymer	Extruder processing parameters				Collector processing parameters		
	Head temperature (°C)	Twist of screws (rpm)	Distance between collector and spinneret (cm)	Spinning voltage (kV)	Air flow rate (Nm ³ /h)	Speed of spindle (rpm)	Speed of oscillation (mm/s)
Moplen HP 462R PP	300	0.1	20, 25, 30, or 35	30	6	11	30
PLA 4060D	170	0.1	20, 25, or 30	30	10	11	30

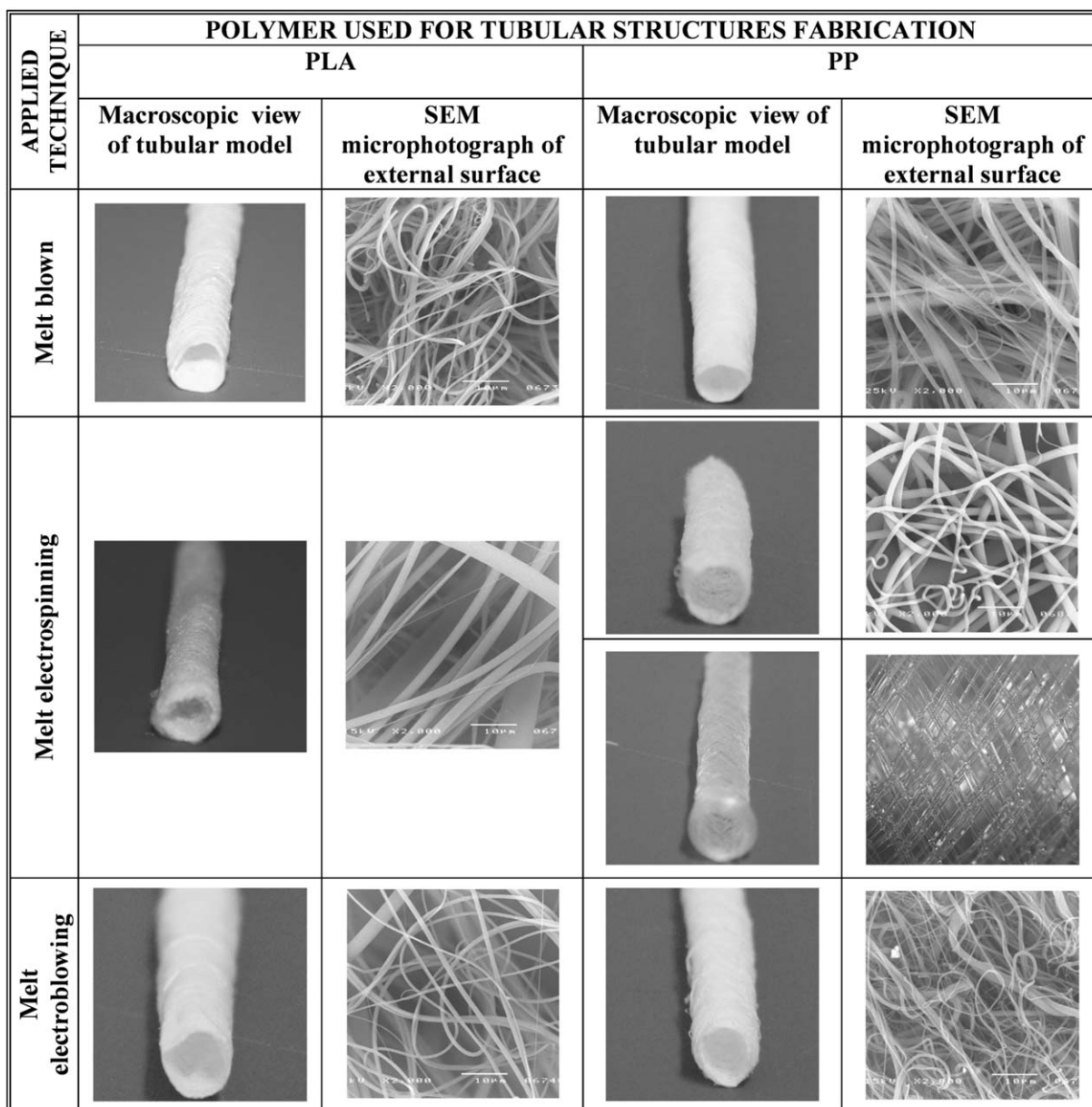


Figure 2. Examples of PLA and PP tubular structures prepared by melt blowing, melt electrospinning, or melt electroblowing technique.

ANALYTICAL METHODS

Fiber Diameter Determination

Scanning Electron Microscopy. A Nova NanoSEM 230 scanning electron microscope (FEI Company/Netherlands) was used to study the morphology of the obtained fibrous structures. More than 15 SEM microphotographs were collected for each tubular structure, and 400–700 fiber diameter measurements were made to obtain a relative error of less than 7% for the average fiber diameter value. The average fiber diameter of the tubular fibrous structures was obtained by analyzing the SEM micrographs using Lucia G image-analysis software.

Structural Properties of Tubular Fibrous Structures

Differential Scanning Calorimetry. Differential scanning calorimetry (DSC) measurements were performed to determine the

polymer thermal characteristics, such as the glass transition temperature (T_g), the cold crystallization temperature (T_c), and the melting temperature (T_m) using a Q2000 device (TA Instruments, USA) calibrated with indium. All measurements were obtained at a heating rate of 10°C/min and within the temperature range of 0–200°C in a dry nitrogen environment according to the PN-EN ISO 11357:2009 Standard.

The enthalpies of crystallization (ΔH_c) and melting (ΔH_m) were measured. The crystallinity index (CI) of the samples was calculated using the following equation:

$$\text{Crystallinity index} = \left[\frac{\Delta H_m - \Delta H_c}{\Delta H_f} \right] \cdot 100; [\%] \quad (1)$$

where, ΔH_f is the theoretical heat of fusion for 100% crystalline PP (207 J/g).²⁷

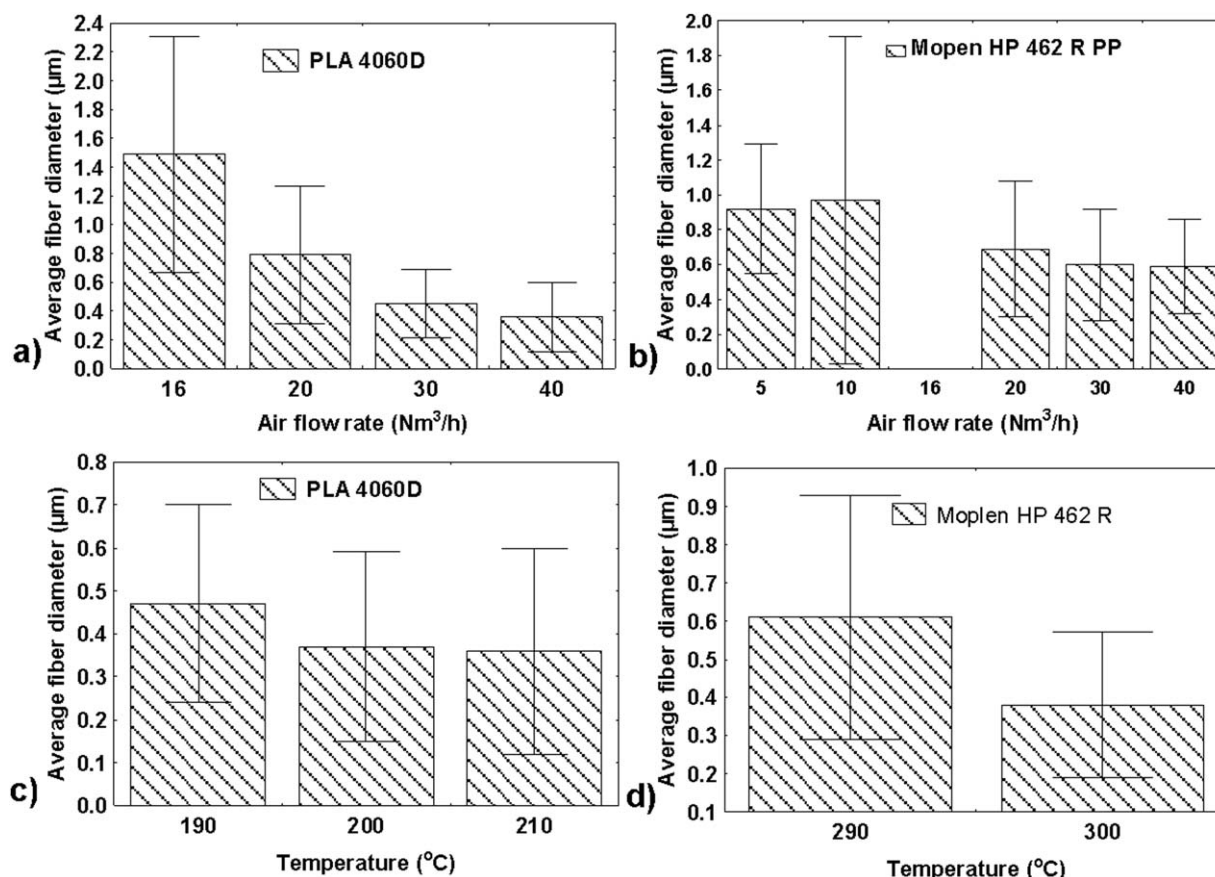


Figure 3. Effect of melt blown processing parameters such as: air flow rate for (a) PLA and (b) PP, extruder head temperature for (c) PLA and (d) PP on the average fiber diameter (The error bars represent standard deviation).

The CI values of the fabricated samples were compared with the values obtained for the native polymers.

FTIR. The spectroscopic measurements of the fabricated fibrous structures were collected using a Nicolet FTIR Spectrometer (Thermo Scientific, USA) with a coupled ATR adapter using “The Thermo Scientific” control unit. The FTIR absorption spectra were collected using an ACD/SpecManager (Thermo Scientific, USA) within a wavelength range of 4000–600 cm^{-1} .

Statistical Data Analysis

Statistical analysis standard deviation (SD), coefficient of variance (CV), and relative error (RE) for the tubular structure fiber diameter were conducted.

RESULTS AND DISCUSSION

Tubular Structure Fabrication

The tubular structures of PLA and PP were produced using melt blowing, melt electrospinning, and melt electroblowing. The processing parameters for tubular fibrous structure fabrication were selected based on the fiber diameter and physiochemical parameter of flat fibrous structures made in previous studies.^{15,18–21} The extruder could not operate at a rate higher than 1 rpm of screws’ twist if the resulting structure was to have as small a diameter as possible. The voltage used for fiber spinning ranged from 30 to 40 kV and was chosen to produce the smallest possible fiber diameter for flat fibrous struc-

tures.^{15,20} Figure 2 shows selected examples of the PLA or PP tubular structures prepared by the three melting techniques.

The melt electrospun tubular structures were constructed from a single fiber crisscrossed winding; a nonwoven structure was also prepared from PP. The difference in structures depended on the melt electrospinning processing parameters, such as extruder temperature and applied voltage. Using a lower extruder temperature (approx. 210°C) and a low spinning voltage (approx. 20 kV) resulted in the cross winding of fibers, whereas the application of a higher temperature (approx. 240°C) and voltage (approx. 30 kV) resulted in the nonwoven structure.

Effect of Processing Parameters on the Fiber Diameter

The influence of processing parameters on the obtained tubular structure fiber diameter for each presented technique was extensively examined.

Melt Blown. The effect of the air flow rate for the melt blown tubular structures was examined. Figure 3(a,b) shows the dependence of air flow rate and the resulting changes in the fiber diameter for samples prepared using constant processing parameters (extruder head temperature: PLA – 190°C, PP – 290°C; working distance: 15 cm). The increase in the air flow rate caused the fiber diameter of the tubular structures to decrease for all polymers. The decrease in fiber diameter was attributed to an increase in the stretching of the formed fibers with an increasing air flow rate.

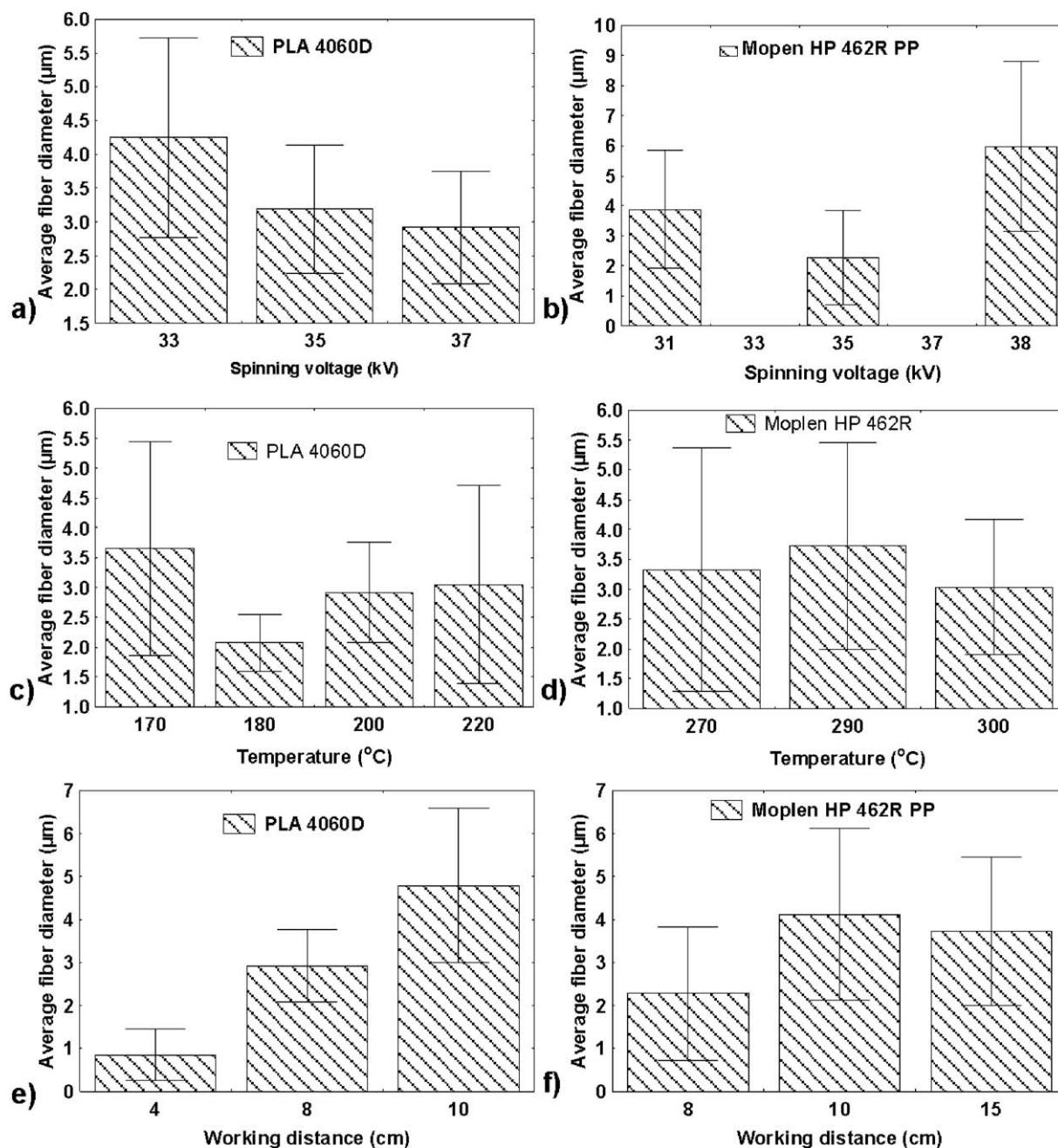


Figure 4. Effect of melt electrospinning processing parameters such as: spinning voltage for (a) PLA and (b) PP, extruder head temperature (c) PLA and (d) PP, working distance (e) PLA, and (f) PP on the average fiber diameter (The error bars represent standard deviation).

The influence of the extruder head temperature on the fiber diameter of the melt-blown tubular structures was also studied. A reduction in fiber diameter with increasing applied extruder head temperature was observed for each studied polymer. The polymer melt flow rate increased with processing temperature and led to a reduction in the fiber diameter. The highest temperature used in this investigation was 220°C for PLA and 300°C for PP.

Figure 3(c,d) shows the relationship between the extruder head temperature and the melt-blown tubular structure fiber diameter at a constant air flow rate (30 Nm³/h) and working distance

(15 cm). The tendency for forming the smallest fiber diameter was observed for PLA and PP if the processing temperature was 220 and 300°C, respectively.

Melt Electrospinning. It was determined that the spinning voltage, the distance from the collector to the spinneret, and the processing temperature had the greatest influence on the average fiber diameter of the melt electrospun structures.^{28–30}

A decrease in fiber diameter was observed when the spinning voltage for PLA and PP was approximately 35 kV. The increase

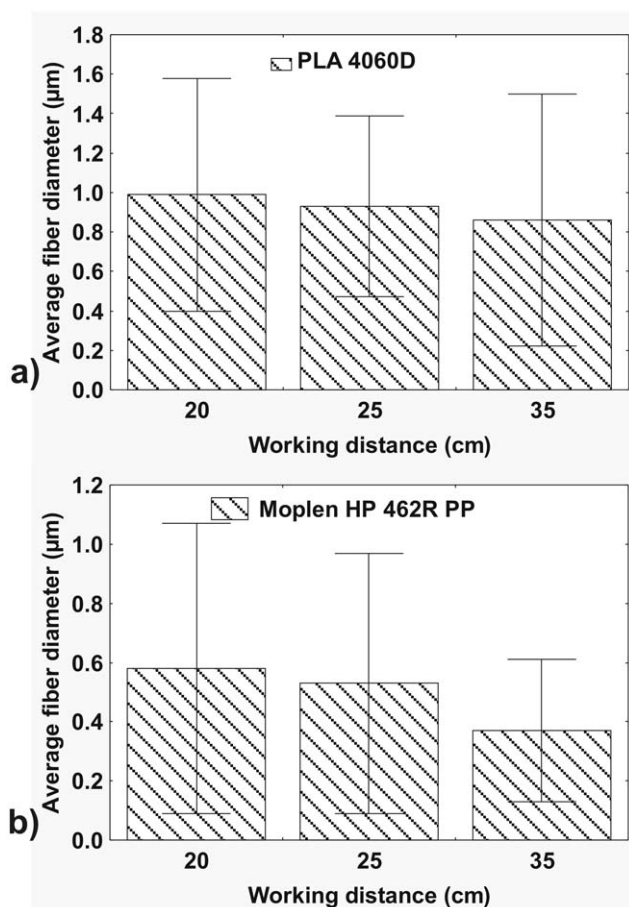


Figure 5. Effect of working distance in the melt electroblowing technique on the fiber diameter tubular structures made of: (a) PLA and (b) PP (The error bars represent standard deviation).

in spinning voltage caused some fluctuation of the electrospinning process. The formed cone of the polymer originated at the spinning head was not stable. Above phenomenon is resulted from too fast pull out of the stream. Taking into account the above phenomenon, the application of 35 kV was not influenced on the reduction of the fiber diameter. Figure 4(a,b) show the dependence of fiber diameter on the spinning voltage samples prepared at constant processing parameters (extruder head temperature: PLA – 220°C, PP – 290°C; working distance: PLA – 8 cm, PP – 15 cm).

The melt electrospinning temperature for each polymer used had the least influence on fiber diameter for the resulting tubular structures. The increase in the temperature of the extruder affected the increase in the MFR of the polymer resulting in the reduction of the fiber diameter. Moreover, above phenomenon is able to effect the loss of electrospinning process stability. Figure 4(c,d) shows the influence of the processing temperature on the melt electrospun tubular structures made of PLA and PP and fabricated at spinning voltages of 37 kV and working distances of 8 and 10 cm, respectively.

The smallest fiber diameters were obtained when the working distance was decreased to 4 cm for each polymer. A shortened distance

between collector and spinneret promoted smaller fiber diameters because of the higher electric field strength. Figure 4(e,f) shows the influence of working distance during the melt electrospinning process on fiber diameter for samples prepared at the aforementioned head temperatures and a spinning voltage of 37 kV.

The smallest fiber diameter was obtained when the tubular structures of both polymers were fabricated at a spinning voltage of 35 kV paired with the highest processing temperature and the shortest working distance.

Combination of Melt Blowing and Electrospinning. A combination of the melt electrospinning and melt blowing techniques was used. The optimal processing parameters for melt electrospinning include low air flow (10 Nm³/h for PLA and 6 Nm³/h for PP) and spinning voltage (30 kV), whereas for the fibers derived from the melt electroblowing process are most influenced by the working distance. The influence of air blowing and electrostatic forces and their effect on the fiber diameter of the resulting structures was studied in this case. Figure 5 shows the influence of working distance during melt electroblowing on the fiber diameter, where an increase in working distance reduced the fiber diameter of the tubular structures. The decrease in the fiber diameter is attributed to the simultaneous increase in the electrostatic force and working distance.

It should be noted that inherently high variability in the fiber diameter distribution depicted by overlapping error bars was observed (Figures 3–5).

The effects of the processing parameters on the PLA and PP fiber diameters of the tubular structures obtained by melt blowing, melt electrospinning, and melt electroblowing are presented in Figure 6.

Minimum and Maximum Fiber Diameter Results

The SEM micrographs reveal distinct examples of tubular structures prepared by melt blowing, melt electrospinning, and melt electroblowing; the smallest and largest average fiber diameters are shown in Figure 7 (PLA tubular structures) and Figure 8 (PP tubular structures).

The PLA tubular structures with the smallest average fiber diameter had the largest CV (the coefficient of variation). This relationship was observed for all the used manufacturing techniques and reveals that an increase in the electric field or air flow rate leads to a larger fiber distribution for the PLA tubular structures.

The PLA melt electrospun tubular structures with an average fiber diameter of $8.12 \pm 2.45 \mu\text{m}$ had the smallest CV (30%). Correspondingly, the PLA melt electroblown tubular structures with an average fiber diameter of $0.86 \pm 0.67 \mu\text{m}$ had the largest CV (78%).

The PP tubular structures with an average fiber diameter of $0.58 \pm 0.49 \mu\text{m}$ obtained by melt electroblowing had the largest CV (84%). Conversely, PP tubular structures with an average fiber diameter of $5.96 \pm 2.83 \mu\text{m}$ obtained by melt electrospinning had the smallest CV (47%).

The same phenomenon was observed for the PP structures except the PP structures made using the melt-blown technique,

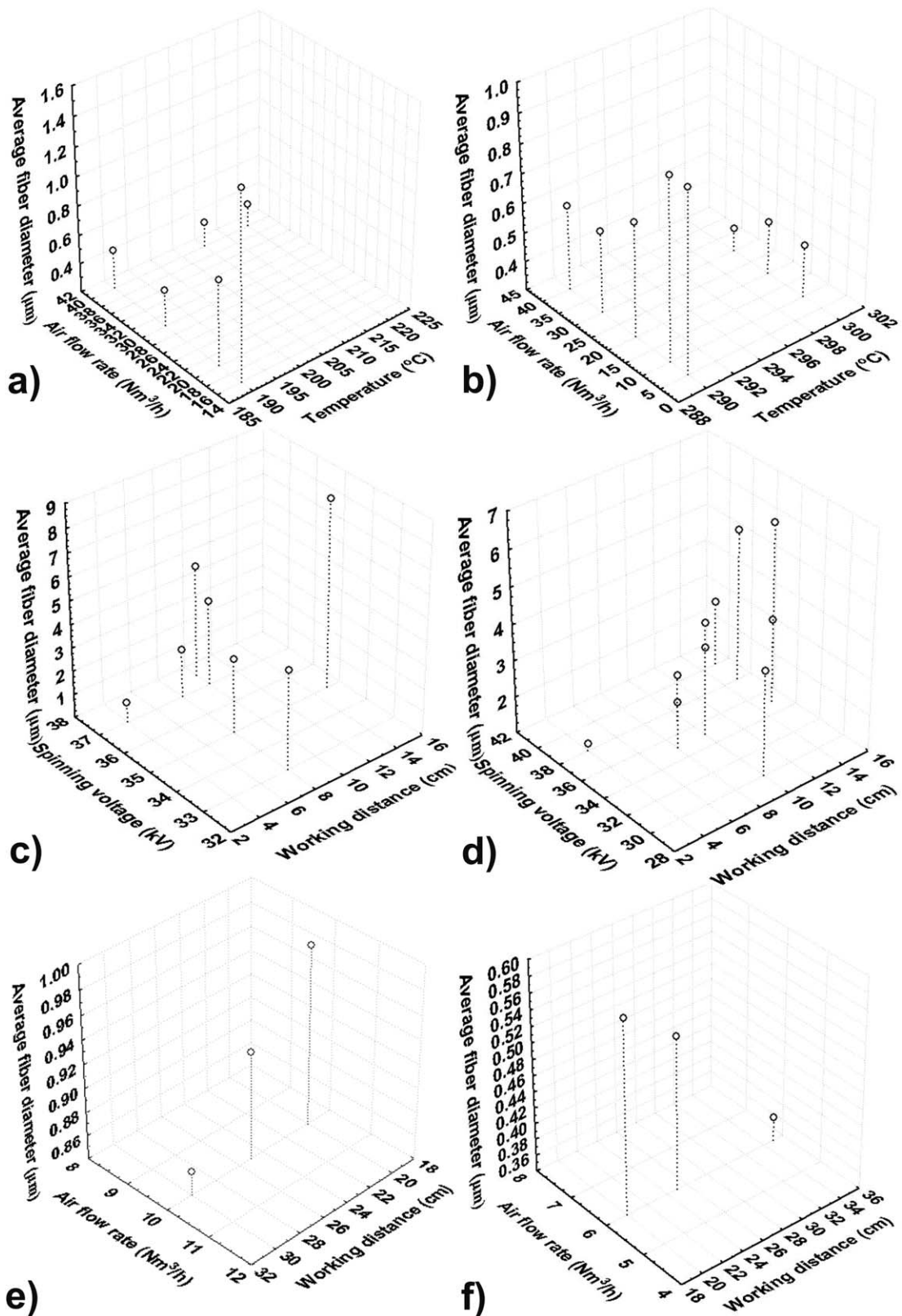


Figure 6. Effect of processing parameters on the average fiber diameter of PLA tubular structures produced using (a) melt blowing, (c) melt electrospinning, (e) melt electroblowing; and the PP tubular structures produced using (b) melt blowing, (d) melt electrospinning, (f) melt electroblowing.

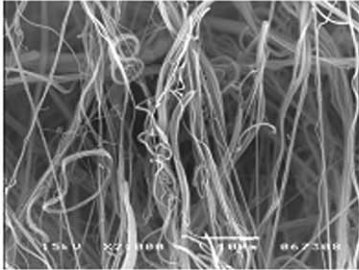
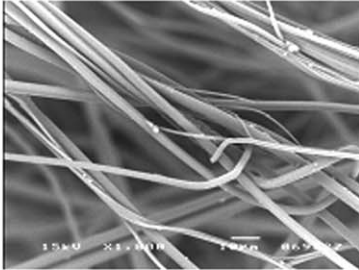
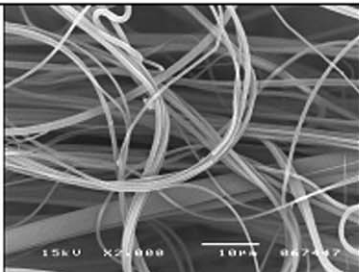
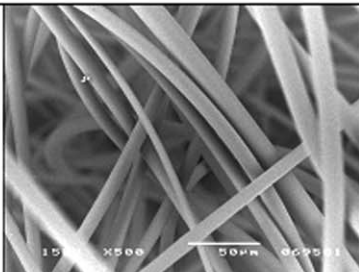
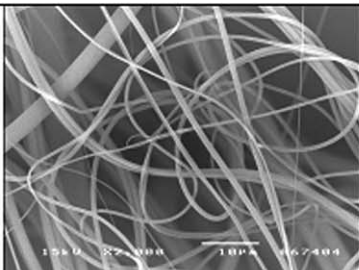
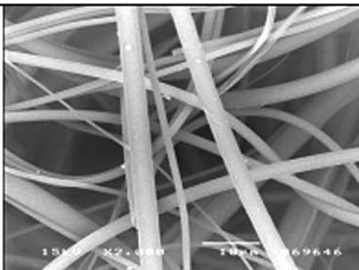
POLYMER USED FOR TUBULAR STRUCTURES FABRICATION: PLA						
Working parameters						
Melt blowing parameters	Temperature of head (°C)	220		220		
	Twist of screws (rpm)	1		1		
	Distance of collector to spinneret (cm)	15		15		
	Air flow rate (Nm³/h)	40		6		
	Speed of spindle (rpm)	30		30		
	Speed of oscillation (mm/s)	6		11		
Melt electrospinning parameters	Temperature of head (°C)	220		220		
	Twist of screws (rpm)	0.1		0.1		
	Distance of collector to spinneret (cm)	4		15		
	Spinning voltage (kV)	37		35		
	Speed of spindle (rpm)	30		30		
	Speed of oscillation (mm/s)	11		11		
Melt electroblowing parameters	Temperature of head (°C)	170		170		
	Twist of screws (rpm)	1		1		
	Distance of collector to spinneret (cm)	30		20		
	Spinning voltage (kV)	30		30		
	Air flow rate (Nm³/h)	10		10		
	Speed of spindle (rpm)	30		30		
	Speed of oscillation (mm/s)	11		11		

Figure 7. SEM micrographs of the PLA tubular structures with ultimate fiber diameters (the smallest or the largest) made from various techniques.

where the lowest CV for the structures having smaller fiber diameter was found.

The application of the melt techniques, and in particular, the suitable selection of the processing parameters yielded in the variation of the fibrous structure behavior, mostly in the fibers diameter and porosity of resulted tubular structures. The appropriate selection of the processing parameters give a possibility

for the fabrication of the tubular prosthesis having structures facility for the relatively quick natural tissue in-growth (tissue integration of the vascular graft).

Structural Properties of Fabricated Tubular Structures

Differential Scanning Calorimetry. The DSC thermographs of the corresponding native polymers and the tubular structures were collected to analyze their thermal characteristics and to

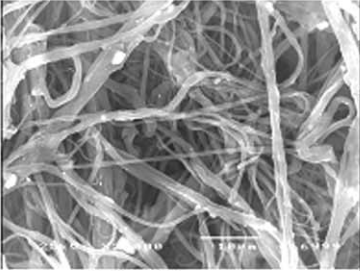
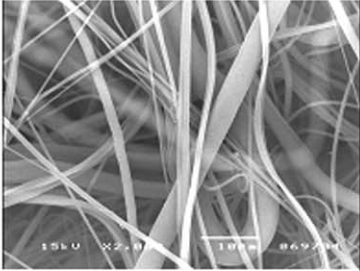
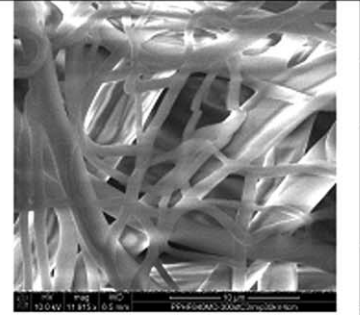
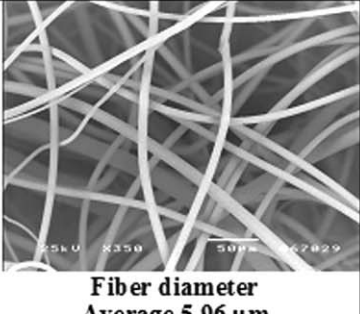
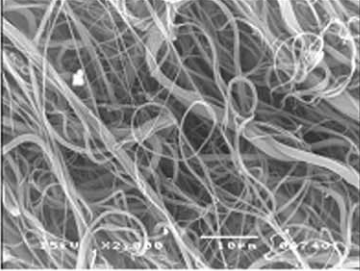
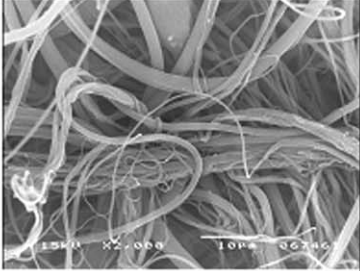
POLYMER USED FOR TUBULAR STRUCTURES FABRICATION: PP							
Melt blown parameters	Working parameters						
	Temperature of head (°C)	290			290		
	Twist of screws (rpm)	0.1			0.1		
	Distance of collector to spinneret (cm)	10			10		
	Air flow rate (Nm ³ /h)	40			10		
	Speed of spindle (rpm)	30			30	Fiber diameter Average 0.38 μm SD ± 0.19 μm CV 49 %	Fiber diameter Average 0.92 μm SD ± 0.82 μm CV 88 %
	Speed of oscillation (mm/s)	11			11		
Melt electrospinning parameters	Temperature of head (°C)	300			290		
	Twist of screws (rpm)	0.1			1		
	Distance of collector to spinneret (cm)	4			15		
	Spinning voltage (kV)	37			38		
	Speed of spindle (rpm)	30			30	Fiber diameter Average 1.21 μm SD ± 1.00 μm CV 82 %	Fiber diameter Average 5.96 μm SD ± 2.83 μm CV 47 %
	Speed of oscillation (mm/s)	11			11		
	Melt electroblowing parameters	Temperature of head (°C)			300		
Twist of screws (rpm)		0.1	0.1				
Distance of collector to spinneret (cm)		35	20				
Spinning voltage (kV)		30	30	Fiber diameter Average 0.35 μm SD ± 0.25 μm CV 67 %	Fiber diameter Average 0.58 μm SD ± 0.49 μm CV 84 %		
Air flow rate (Nm ³ /h)		6	6				
Speed of spindle (rpm)		30	30				
Speed of oscillation (mm/s)		11	11				

Figure 8. SEM micrographs of the PP tubular structures with ultimate fiber diameters (the smallest or the largest) made from various techniques.

determine the changes in structural properties during polymer processing.

Two samples made from melt blown, melt electrospun or melt electroblown tubular structures were used for the DSC analysis.

The DSC study was performed for melt blown structures manufactured at high (40 Nm³/h for both polymers) and low (10 Nm³/h for PLA and 5 Nm³/h for PP) air flow rate, whereas the melt electrospun samples manufactured at high (5 kV/cm for

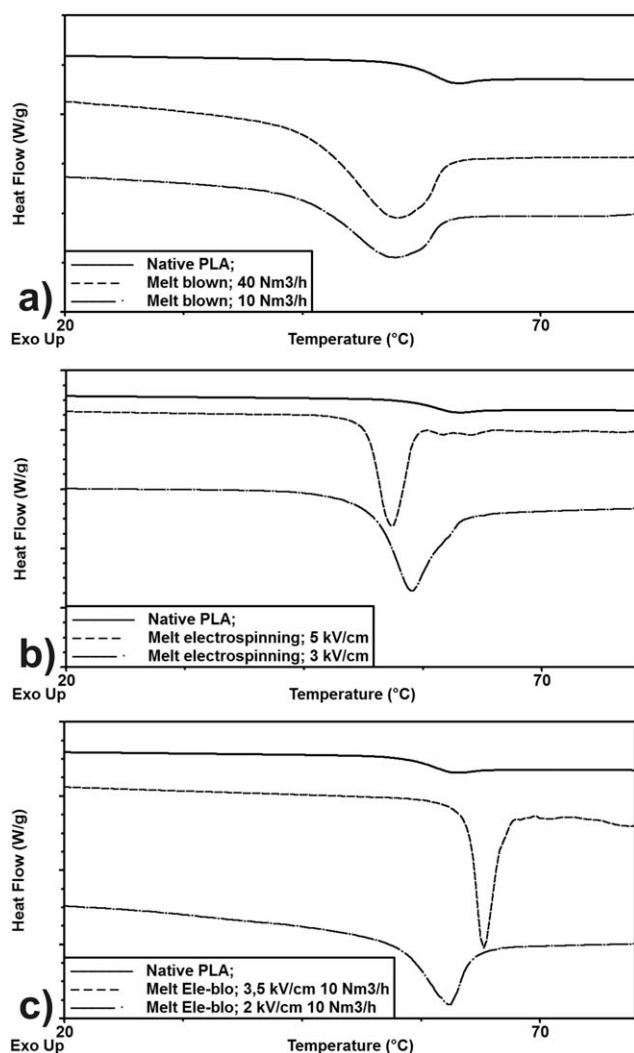


Figure 9. Comparison of the DSC thermographs for the native PLA and resulting tubular fibrous structures made using (a) melt blowing; (b) melt electrospinning; (c) melt electroblowing.

PLA and 6.7 kV/cm for PP) and low (3 kV/cm for PLA and 2.3 kV/cm for PP) electric field were selected. Moreover, the melt electroblown structures prepared at constant air flow rate (10 Nm³/h for PLA and 6 Nm³/h for PP) and variable electric field were also selected.

The thermographs of the amorphous PLA show only the glass transition temperature (T_g). For the native amorphous PLA, the glass transition temperature was detected at 59°C. The T_g of the native PLA and its tubular structures are presented in Figure 9, whereas the comparison of the glass transition temperature for the native polymer and tubular fibrous structures is shown in Table II. The melt blown, melt electrospun, and melt electroblown processes did not form crystalline PLA structures as shown in Figure 9. The differences in the DSC thermographs for the PLA tubular structures obtained by the melt blowing and electrospinning process are most likely the result of a high electrical charge used on the polymer melt at the solidification phase in the melt electrospinning process [Figure 9(a,b)]. The magnitude of the T_g relaxation peak increased for the melt elec-

trospun PLA tubular structures. The larger area under the T_g peak for these structures is a consequence of the molecules exhibiting a longer overall relaxation time.³¹ The same effect is detected in DSC thermographs for PLA melt electroblown tubular structures. The application of a higher electric field for PLA processing caused similar changes in the T_g peak area.

The thermal analysis of the native PP presents only the melt temperature (T_m) detected at 163°C. All examined samples for each manufacturing technique show an endothermic peak at approximately 160°C. The thermal behavior of native PP and its tubular structures is presented in Figure 10.

Table III presents a comparison of T_m and CI for each processed PP sample and native PP. There is no change in the melting temperature of the native PP and its tubular structure. The changes in the enthalpy of fusion and the crystallinity index of PP were studied. The crystallinity index for PP tubular structures prepared by melt blowing, melt electrospinning, and melt electroblowing showed similar values. However, the fabrication process yielded an increase in the CI of approximately 44% compared with 29% CI for the native polymer.

FTIR. The FTIR spectra were collected for the melt-blown, melt electrospun, and melt electroblown tubular structures made of PLA and PP. For each tubular structure manufacturing method, two variants of the obtained structures were analyzed. The tubular structures prepared at high (40 Nm³/h for both polymers) and low (10 Nm³/h for PLA and 5 Nm³/h for PP) air flow rates for the melt blowing process were collected for analysis; for melt electrospinning, the specimens were collected at high (5 kV/cm for PLA, 6.7 kV/cm for PP) and low (3 kV/cm for PLA, 2.3 kV/cm for PP) electric field, whereas the melt electroblowing specimens were collected at constant (10 Nm³/h for PLA and 6 Nm³/h for PP) air flow rate and a varying electric field.

Sample selection was performed based on the influence of selected processing parameters for each manufacturing technique based on the structural properties of the tubular structure.

There were no changes in FTIR spectra between the raw materials and the processed polymers. Then, only some examples of the FTIR spectra will be described. Figure 11(a,c,e) shows the FTIR spectra of the PLA tubular structures prepared by the

Table II. Comparison of the Glass Transition Temperature for the Native PLA and Resulting Tubular Fibrous Structures Made Using Melt Electrospinning, Melt Blowing, and Melt Electroblowing

Processing method; parameters	T_g (°C)
Native	59
Melt electrospinning; 5 kV/cm	53
Melt electrospinning; 3 kV/cm	55
Melt blown; 40 Nm ³ /h	51
Melt blown; 10 Nm ³ /h	51
Melt electroblowing; 3.5 kV/cm, 10 Nm ³ /h	63
Melt electroblowing; 2 kV/cm, 10 Nm ³ /h	58

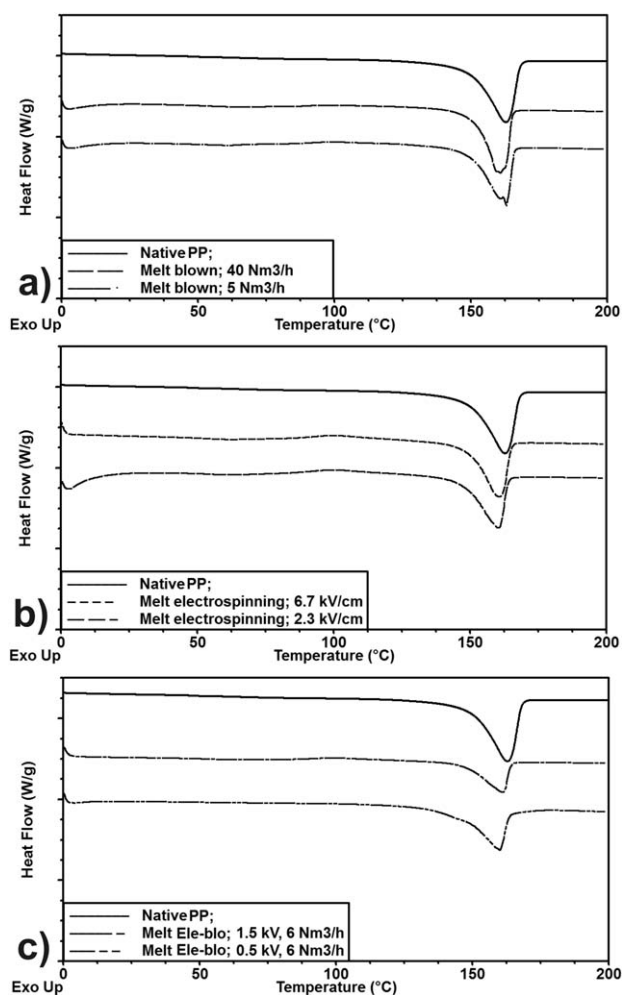


Figure 10. Comparison of the DSC thermographs for the native PP and resulting tubular fibrous structures made of using (a) melt blowing; (b) melt electrospinning; (c) melt electroblowing.

melt blowing, melt electrospinning, and melt electroblowing techniques. The specific absorption bands of PLA are also indexed in the displayed FTIR spectrum. The FTIR spectra did not show any differences in the absorption bands between the structures prepared at high or low air flow rate or for high or low electric field. These results indicate that the changes in air flow rate or electric field did not influence the chemical structure of PLA.

Figure 11(b,d,f) shows the examples of FTIR spectra of PP tubular structures prepared by the three investigated methods. The selection of the tubular structures was similar as for PLA. The specific absorption bands of PP are displayed in the presented FTIR spectra. Similar to that of PLA, the FTIR spectra of the PP tubular structures did not show changes between structures obtained under different processing parameters.

Moreover, the FTIR spectra of the tubular structures prepared by melt blowing, melt electrospinning, or melt electroblowing indicated similar absorption bands, confirming that the processing method has no effect on the structural properties of designed tubular textile structures. No oxidation was observed,

suggesting that the nonconventional textile techniques are non-destructive for the processing of PLA and PP. The above-mentioned phenomenon can be similarly explained by the polymer processing—melting, which was used in all the applied techniques; the air flow rate and electric field rate did not influence the chemical structures of the produced tubular structures.

CONCLUSION

During the presented research, the influence of processing parameters on the average fiber diameter for each manufacturing technique was extensively investigated. The increase in the air flow rate and extruder head temperature effected on the reduction of the melt blown structures fiber diameter. In melt electrospinning process, the strongest effect of the working distance and applying the spinning voltage about 35 kV on decrease of the fiber diameter have been noticed. However, the reduction of fiber diameter with the increase in the working distance for the melt electroblowing process was observed.

The smallest fiber diameter for the PLA and PP tubular structures was obtained for the melt blown structures (PLA – average fiber diameter: approximately $0.60 \pm 0.40 \mu\text{m}$; PP – average fiber diameter: approximately $0.38 \pm 0.19 \mu\text{m}$).

It was possible to obtain the small fiber diameter for the tubular structures by applying only a high voltage. The smallest average fiber diameter for melt electrospun PLA tubular structures, which was obtained under high voltage and without compressed air application, was approximately $0.85 \pm 0.6 \mu\text{m}$. Under the same conditions, the smallest fiber diameter for the melt electrospun PP tubular structures was approximately $1.22 \pm 1.00 \mu\text{m}$.

The parameters of the fabrication processes had an influence on the received fiber diameters and then the final physical properties of the tubular structures. The increase in the spinning voltage above 35 kV caused the fluctuation of the cone stream and the lack of the subsequent reduction in the fiber diameter. The DSC and FTIR analyses confirmed that processing parameters, such as air flow rate and/or electric field, did not have influence on the structural properties of the produced tubular forms, both for PLA and PP polymers.

Table III. Comparison of the Melt Temperature and CI for the Native PP and Tubular Fibrous Structures Made Using Melt Electrospinning, Melt Blowing, or Melt Electroblowing

Processing method; parameters	T_m (°C)	Crystallinity index (CI) %
Native	163	29
Melt electrospinning; 6.7 kV/cm	161	44
Melt electrospinning; 2.3 kV/cm	160	43
Melt blown; 40 Nm ³ /h	163	44
Melt blown; 5 Nm ³ /h	161	46
Melt electroblowing; 1.5 kV/cm, 6 Nm ³ /h	161	43
Melt electroblowing; 0.5 kV/cm, 6 Nm ³ /h	160	42

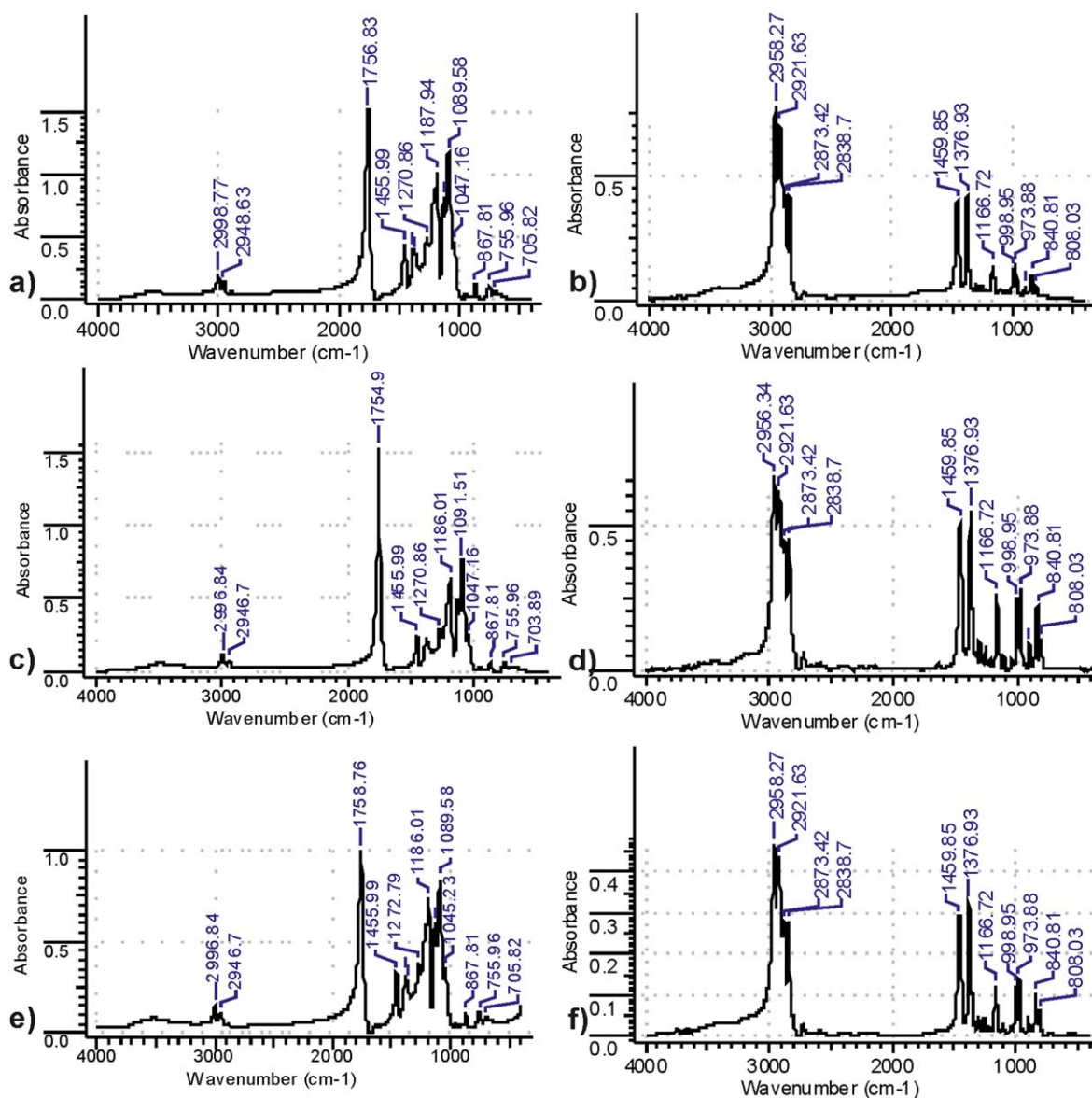


Figure 11. Examples of FTIR spectra of PLA processed by: (a) melt electrospinning; (c) melt blowing, and by (e) melt electroblowing and example FTIR spectra of PP processed by (b) melt electrospinning; (d) melt blowing, and by (f) melt electroblowing. [Color figure can be viewed in the online issue, which is available at wileyonlinelibrary.com.]

The proposed selection of the processing parameters of melt techniques used in the study allows for the designing process for the fabrication of the tubular structures being the models of the vascular prosthesis. The changes in the structural properties during the main fabrication process allow to select the most optimal processing parameters resulting in the structures having the relatively high crystallinity, the main parameters affecting the high biological resistance of the nonbiodegradable polymers.

The structural properties of the resulted structures are the main inputs for the biocompatibility studies, mostly biodegradation tests, allowing to explain the effect of the biological degradation of the final multilayered semidegradable prosthesis.

The next stage of research will be the analysis of the effect of fabrication technique used on the mechanical and physical properties of resulted tubular structures, and then the selection

of appropriate technology for multilayered tubular structures design.

ACKNOWLEDGMENTS

The current work is performed within the framework of the project titled “Biodegradable fibrous products” (acronym: Biogratex) supported by the European Regional Development Fund; Agreement No. POIG.01.03.01-00-007/08-00.

REFERENCES

- Wilson, C. T.; Fisher, E. S.; Welch, H. G.; Siewers, A. E.; Lucas, F. L. *Health Aff. Millwood*. **2007**, *26*, 162.
- Rabkin, E.; Schoen, F. *Cardiovasc. Pathol.* **2002**, *11*, 305.

3. Hoerstrup, S. P.; Zünd, G.; Sodian, R.; Schnell, A. M.; Grünenfelder, J.; Turina, M. I. *Eur. J. Cardiothorac. Surg.* **2001**, *20*, 164.
4. Sarkar, S.; Salacinski, H. J.; Hamilton, G.; Seifalian, A. M. *Eur. J. Vasc. Endovasc. Surg.* **2006**, *31*, 627.
5. Soldani, G.; Panol, G.; Sasken, H. F.; Goddard, M. B.; Galletti, P. M. *J. Mater. Sci. Mater. Med.* **1992**, *3*, 106.
6. Hadjizadeh, A.; Ajji, A.; Bureau, M. N. *J. Mech. Behav. Biomed.* **2010**, *3*, 574.
7. Gulbins, H.; Dauner, M.; Petzold, R.; Goldemund, A.; Anderson, I.; Doser, M.; Meiser, B.; Reichart, B. *J. Thorac. Cardiovasc. Surg.* **2004**, *128*, 372.
8. Moreno, M. J.; Ajji, A.; Mohebbi-Kalhor, D.; Rukhlova, M.; Hadjizadeh, A.; Bureau, M. N. *J. Biomed. Mater. Res. B Appl. Biomater.* **2011**, *97*, 201.
9. Krucińska, I.; Komisarzczyk, A.; Chrzanowski, M.; Paluch, D. *FIBRES TEXT. East. Eur.* **2007**, *15*, 64.
10. Błasińska, A.; Krucińska, I.; Chrzanowski, M. *FIBRES TEXT. East. Eur.* **2004**, *12*, 51.
11. Chung, S.; Ingle, N. P.; Montero, G. A.; Kim, S. H.; King, M. W. *Acta Biomater.* **2010**, *6*, 1958.
12. Kim, J. S.; Jang, D. H.; Park, W. H.; Min, B. M. *Polymer* **2010**, *51*, 1320.
13. Brown, T. D.; Slotosch, A.; Thibaudeau, L.; Taubenberger, A.; Loessner, D.; Vaquette, C.; Dalton, P. D.; Huttmacher, D. W. *Biointerphases* **2012**, *7*, 1.
14. Karchin, A.; Simonovsky, F. I.; Ratner, B. D.; Sanders, J. E. *Acta Biomater.* **2011**, *7*, 3277.
15. Mazalevska, O.; Struszczyk, M. H.; Chrzanowski, M.; Krucińska, I. *FIBRES TEXT. East. Eur.* **2011**, *19*, 4, 46.
16. One Lee, B.; Anko, J.; Won Han, S. *Adv. Mater. Res.* **2010**, *123*, 935.
17. Rajkishore, N.; Rajiv, P.; Illias, L. K.; Yen, B. T.; Lyndon, A. *Text. Res. J.* **2012**, *82*; DOI: 10.1177/0040517511424524.
18. Mazalewska, O.; Struszczyk, M. H.; Chrzanowski, M.; Krucińska, I. XIV Scientific Conference of Faculty of Material Technologies and Textile Design. Lodz University of Technology, Lodz; **2011**.
19. Mazalewska, O.; Struszczyk, M. H.; Chrzanowski, M.; Krucińska, I. XIV Scientific Conference of Faculty of Material Technologies and Textile Design 2012. Lodz University of Technology, Lodz; **2012**.
20. Mazalevska, O.; Struszczyk, M. H.; Krucińska, I. *J. Appl. Polym. Sci.* **2012**; DOI:10.1002/app.38818.
21. Krucinska, I.; Struszczyk, M. H.; Mazalewska, O. Patent Application RP No. P3998860; **2012**.
22. Homopolymer Moplen, Technical Data Sheets. Available at: <http://www.basellorlen.pl/inside.php?pg=db9ad57c5539d4433be69e3754569b24&>. Accessed February 11, 2013.
23. Huttmacher, D. W. *J. Biomater. Sci. Polym. Ed.* **2001**, *12*, 107.
24. Kim, B. S.; Mooney, D. J. *J. Biomech. Eng.* **2000**, *122*, 210.
25. Krucińska, I.; Surma, B.; Chrzanowski, M.; Skrzetuska, E.; Puchalski, M. *Text. Res. J.* **2012**; DOI: 10.1177/0040517512460293.
26. NatureWorks® PLA Polymer 4060D, For Heat Seal Layer in Coextruded Oriented Films. Available at: <http://www.unicgroup.com/upfiles/file01170656427.pdf>. Accessed May 8, 2012.
27. Cheng, S. Z. D.; Janimak, J. J.; Zhang, A. Q.; Hsieh, E. T. *Polymer* **1991**, *32*, 648.
28. Liu, Y.; Deng, R.; Hao, M.; Yan, H.; Yang, W. *Polym. Eng. Sci.* **2010**, *50*, 2074.
29. Klee, K.; Möller, D. *Polymer* **2007**, *48*, 6823.
30. Lyons, J.; Li, Ch.; Ko, F. *Polymer* **2004**, *45*, 7597.
31. Sichina W. I. Measurement of Tg by DSC. Available at: http://www.metrotec.es/metrotec/WWW_DOC/PETech-09.pdf. Accessed April 6, 2013.